Scattering Effect Based on Measurements of Reflection Coefficients at 60 GHz in an Underground Mine Gallery

Shah Ahsanuzzaman Md Tariq*, Charles Despins†, Sofiène Affes‡ and Chahé Nerguizian*

*École Polytechnique de Montréal, Montreal, Canada
†PROMPT-Quebec, Montreal, Canada
‡INRS-EMT, Université du Québec, Montreal, Canada
Emails: tariq.shah-ahsanuzzaman-md@polymtl.ca, CDespins@promptinc.org,
affes@emt.inrs.ca, chahe.nerguizian@polymtl.ca

Abstract—**This paper presents reflection coefficient measurements in order to analyze the scattering effect of rough walls and floor on mm-Wave propagation at 60 GHz in an underground mine. A 60 GHz frequency domain measurement system with directional antennas is considered. Reflection coefficients are obtained by individual reflected signals and line of sight (LOS) signals with a particular reflective angle then compared with theoretical models. Results suggest a distinguishable reflection and scattering characteristics between mine wall and floor. In specular directions, the path loss difference between the LOS and the reflected signal lies between 11 dB to 18 dB. In both surfaces, strong reflections on specular directions and scattering on non specular directions have been observed. Moreover, wall surface of the mine produces more scattering with strong reflections than floor surface. These reflection coefficient parameters are useful to estimate multipath signal strength in channel modelling for propagation prediction in underground mine.**

Index Terms—**60 GHz propagation measurements, reflection coefficients, scattering.**

I. INTRODUCTION

In the last few years, the demand of 60 GHz unlicensed band for Wireless Local Area Network (WLAN) is increasing due to the high speed (i.e. Gbps) multimedia communication in home and commercial environments [1]. The special characteristics of this band, e.g., 57-64 GHz, such as high absorption loss and less interference during propagation, enable improved frequency reuse compared to lower-frequency bands. Besides, in niche markets such as underground mines, automation and security requirements are further driving to the development of 60 GHz wireless communication systems. To develop WLAN system with a 5 mm wavelength, however, the characteristics of propagation reflection and scattering phenomena (e.g., due to the high roughness of the mine gallery surfaces that may cause a non-negligible multipath contribution) must be investigated. Indeed, reflection coefficients are key to the design a scattering channel model in an underground mine with rough surfaces.

To the best of our knowledge, only few experimental investigations of reflection characteristics of interior and exterior homes and office buildings at different frequencies have been published [2]–[8]. Earliest experimental study of reflection, scattering and transmission characteristics of building materials at 60 GHz by Langen *et al*. [6] demonstrated the measurement procedures and exhibited power dependent scattering of building materials. Also noted that, depending on the reflection profile shapes, either Fresnel model or the multiple reflection model can be proposed. Another measurement campaign has been conducted in an office building by Sato *et al*. [5] at 60 GHz frequency and results have been compared with multilayer dielectric models. Measurements of common flooring materials have been carried out in [4] to analyse the frequency dependencies on the reflection coefficients of the materials. Recently, Zhao *et al*. [3] reported measurements of outdoor mm-Wave cellular communications at 28 GHz in New York city and found that outdoor building materials are more reflective (reflection coefficient of 0.896 for tinted glass at $10°$ incident angle) than indoor ones. Moreover, it was reported in [7] and [8] that, multipath reflections from buildings caused at least 15 dB additional pathloss over line of sight signals against 15 to 20 dB in office environments. Some works with the wireless channel characterization at 60 GHz in underground mine has been done in [9], however, no experimental investigation of the reflection coefficients for propagation in underground mines has been reported so far. The objective of this paper is to study of the scattering phenomena of the mine floor and the wall surfaces relative to the reflection coefficients.

This paper is structured as follows: in Section II, different reflection and scattering models are introduced. Experimental setup and the measurement campaign are exposed in section III. Section IV presents the measurement results and analysis. Finally conclusions are given in Section V.

II. REFLECTION MODELS

Since the underground mine surface is rough and the wavelength (λ) is 5 mm, a single reflection or multiple reflections can be present during interaction of electromagnetic (EM) wave to the mine surface. A schematic illustration of the
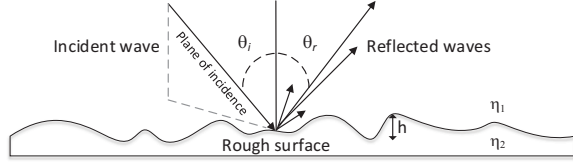
Fig. 1. Rough surface reflection geometry.

multiple reflections, e.g. refers as scattering geometry, is given in Fig 1, where θ_i is the incident angle and θ_r is the specular reflected angle.

A. Fresnel Model

The Fresnel reflection coefficients (Γ) for smooth surfaces provide only the specular reflections. They are related to the material properties, which depend on the incident angle (θ_i), the polarization (vertical, horizontal) and the frequency defined as [2], [10]

$$\Gamma_\parallel = \frac{\eta_2 \cos\theta_t - \eta_1 \cos\theta_i}{\eta_2 \cos\theta_t + \eta_1 \cos\theta_i}$$
$$\Gamma_\perp = \frac{\eta_2 \cos\theta_i - \eta_1 \cos\theta_t}{\eta_2 \cos\theta_i + \eta_1 \cos\theta_t} \quad (1)$$

The E-field component that is parallel to the plane of incidence which has vertical polarization of an antenna refers as parallel reflection coefficient ($\Gamma_\parallel$), whereas the E-field which is perpendicular to the incident plane has horizontal polarization of an antenna and is defined as perpendicular reflection coefficient ($\Gamma_\perp$). The wave impedances ($\eta_{1,2}$) and the transmitted wave angle (θ_t) are expressed in [2].

B. Gaussian rough surface scattering Model

The rough surface produces diffuse reflection, in which incident energy is distributed over the specular direction as described in [10], [11]. Giving the critical height (h_c) of the surface, the dependency on the surface roughness can be defined by the Rayleigh criterion as $h_c = \lambda/(8\cos\theta_i)$. When the height ($h$) of a given rough surface is defined as the minimum to maximum surface protuberance, as shown in Fig. 1, it is considered smooth if $h < h_c$ and rough if $h > h_c$. In the considered underground mine, h is used to be greater than 1 cm which implies a environment with rough surface. Then, the scattering loss factor (ρ_s) [2] with the standard deviation of surface heights (σ_h) will be given by

$$\rho_s = \exp\left[-8\left(\frac{\pi\sigma_h \cos\theta_i}{\lambda}\right)^2\right] \quad (2)$$

C. Modified Gaussian rough surface scattering Model

The scattering loss factor ρ_s is reported in [10] as modified Gaussian rough surface scattering loss factor given by

$$\rho_{sm} = \exp\left[-8\left(\frac{\pi\sigma_h \cos\theta_i}{\lambda}\right)^2\right] I_0\left[8\left(\frac{\pi\sigma_h \cos\theta_i}{\lambda}\right)^2\right] \quad (3)$$

where $I_0(z)$ is the modified Bessel function of zero$^{\text{th}}$ order.

D. Kirchhoff scattering Model

Beckmann and Spizzichino derive an analytical description of the electromagnetic field scattered from a rough surface [11] with the assumption of a Gaussian height distribution. Such surface is characterized by its σ_h and surface correlation length T. Knowing the angles θ_1, θ_2 and θ_3, the average scattering coefficient is given, for a roughness factor g equal or less than 1, by

$$\rho_k = \mathrm{e}^{-g} \cdot \left(\rho_0^2 + \frac{\pi T^2 F^2}{A} \sum_{m=1} \frac{g^m}{m!m} \mathrm{e}^{-\frac{v_{xy}^2 T^2}{4m}} \right) \quad (4)$$

Where $A = l_x \times l_y$ is the surface area. The values of l_x and l_y of the scattering surface have to be chosen large compared to the values of λ and T. ρ_0^2 describes the scattering in specular direction and the second term of (4) is defined as the diffuse scattering. Other parameters of (4) are described in [11]. The Rayleigh roughness factor g is an indicator for the relative surface roughness at a given wavelength, which is given as

$$g = k^2 \sigma_h^2 (\cos(\theta_1) + \cos(\theta_2))^2 \quad (5)$$

It has to be noted that the value of σ_h, T and λ are related to each other through (4) and (5). If σ_h is low and T is high, then the value of g will be less than or equal to 1 which produces specular reflections.

The Gaussian rough surface scattering model, modified Gaussian rough surface and Kirchhoff scattering model are defined when ρ_s, ρ_{sm} and ρ_k are used to modify the Fresnel reflection coefficients, given by

$$\{\Gamma_\parallel, \Gamma_\perp\}_{rough} = \{\rho_s, \rho_{sm}, \rho_k\} \cdot \{\Gamma_\parallel, \Gamma_\perp\} \quad (6)$$

III. EXPERIMENTAL SETUP AND PROCEDURE

A measurement campaign in a static condition, has been carried out at 70 m level in the CANMET mine located in Val d'Or, Quebec. The 70 m gallery, which is narrow in dimension, has a height of 3.5 m and width of 3 m. Digital photographs of measurement campaigns of the floor and the wall of that gallery are shown in Figs. 2 and 3. The measurement point of the reflection coefficient on the floor was mostly covered with small rock tiles (dimension was approximately less than 1 cm and the form like crystal and round) and was wetted, covered with mud and mostly flatted. For the wall, which was entirely less wetted with rough surface in which the rock shape form consists like plates with large heights (average 20 cm) and sharp edges. The gallery was dusty and the humidity was around 100 percent. The temperature was between 6° C and 7° C. Large machinery noise caused by the air ventilation system was also observed in the gallery.

A. Setup

In order to find channel impulse responses, a 60 GHz frequency domain wideband measurement system setup has been used. A Vector Network Analyzer (ANRITSU MS 4647A) with a frequency band ranging from 40 MHz to 70 GHz has been employed. Gain of 30 dB for the Power Amplifier
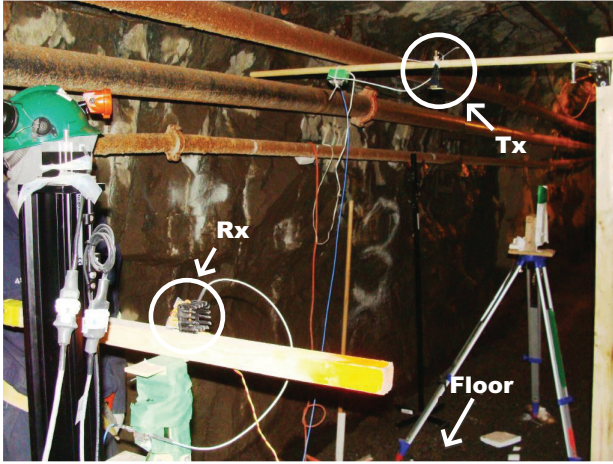
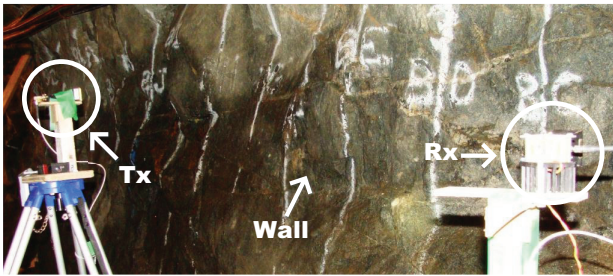Fig. 2. Reflection measurement champaign of the floor.

Fig. 3. Reflection measurement champaign of the wall.

(CBM 57653/015-03 CERNEX), in conjunction with Low Noise Amplifier (CBL 57653/055-01 CERNEX) have been considered. A second Low Noise Amplifier (QuinStar, Serial N11328, Model 001001) has been added, with a gain of 18 dB, to enhance the signal. Directional horn antennas with 24 dBi and half-power beam width (HPBW) of around $12°$ in azimuth and in elevation planes were used for the transmitter (Tx) and the receiver (Rx). The frequency range has been selected from the IEEE Standard 802.15.3c which considers a central frequency channel between 57.24 GHz to 59.4 GHz. The transmit power was set at 4 dBm. For the setup configurations, the system noise floor was -107 dBm. The system calibration was done with 2000 sweep points for the whole bandwidth of 2.16 GHz with a spacing of 1.08 MHz. In order to have accurate and fixed position for the transmitter and the reflection points, a pointing laser with a camera tripod was used. Transmitter and receiver heights were around 1.42 m. The data acquisition was completed by connecting a computer to the VNA via a GPIB interface. A Labview program was employed to control the whole measurement procedure.

B. Procedure

A measurement procedure was carried out to find reflection characteristics in a particular reflected angle. The reflection profile has been measured with a defined test area of the underground mine floor and wall using two step processes, as depicted in Figs. 4 and 5. For a particular incident angle, the first step consisted of recording the frequency response of
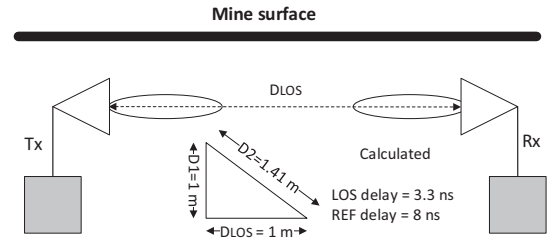

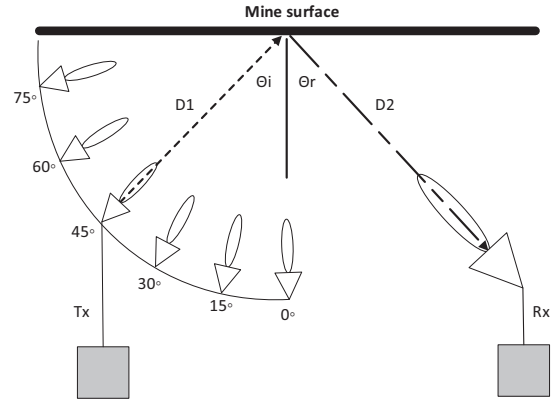Fig. 4. Illustration of the Line of sight signal measurement procedure.

Fig. 5. Illustration of the reflected signal measurement procedure.

the line of sight (LOS) signal as shown in Fig. 4. Secondly, the frequency response of the reflected signal (REF) from the surface point was recorded as shown in Fig 5, in which Rx remained fixed and the Tx moved from $0°$ to $75°$ with a step of $15°$ keeping the distance $(D_1 + D_2)$ constant. D_1 and D_2 are the distances between Tx and the surface point and between the surface point to Rx, respectively. In order to make a far field region of the horn antennas, Tx and Rx were set with a separation of at 1 m. For the floor measurements, Rx was fixed with a wood at an angle of $60°$ and the Tx was vertically moved. For the wall measurements, the Rx remained fixed at $45°$ angle and the Tx was moved horizontally, and Tx and Rx were placed 1 m away from the wall. Tx and Rx positions and incident angles were assumed to be fairly accurate during measurements due to mechanical and automatic movement apparatus constraints. Physical distances $D1$, $D2$ and D_{LOS} were measured from the site in order to verify with recorded propagation delays.

IV. MEASUREMENT RESULTS

Measurements were performed for perpendicular (horizontal antenna polarization) and parallel (vertical antenna polarization) polarizations for the floor and wall surfaces. For each incident angle, an average of 10 LOS and 10 REF channel impulse responses have been recorded. For the post processing of the measured data, LOS and reflected channel impulse responses are shifted by 1 m reference measurement delay, samples for perpendicular polarization for the wall surface are given in Figs. 6 and 7. Fig. 6 shows a delay of 0.46 ns for LOS measurement at $0°$ and a delay of 3.2 ns at $45°$. The delay of reflected signal with all incident angles remains almost fixed
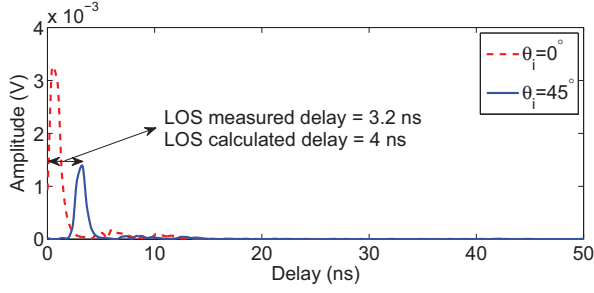
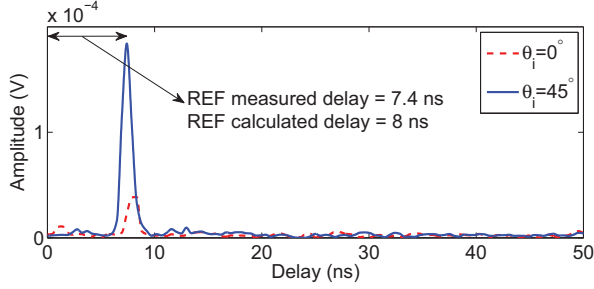Fig. 6. Channel impulse response of LOS signal for the wall surface.

Fig. 7. Channel impulse response of REF signal for the wall surface.

TABLE I
COMPARISON OF REFLECTION COEFFICIENTS OF WALL AND FLOOR.

Surface	$|\Gamma_\parallel|$		$|\Gamma_\perp|$	
	Fresnel	Measured	Fresnel	Measured
Wall ($\theta_i = 45°$)	0.247	0.1267	0.536	0.2445
Floor ($\theta_i = 60°$)	0.155	0.1389	0.691	0.2656

Note: ε, σ for the floor (limestone [2]) and the wall (Granite [6]) are assumed as 7.51, 0.03 S/m and 5.5, 0.215 S/m, respectively.

values between 7.4 ns to 7.8 ns. LOS and REF delays were compared with calculated physical delays and agreed fairly. Moreover, those delays are being used to calculate measured distances D_1, D_2 and D_{LOS} to find $|\Gamma|$. Fig. 7 shows the maximum amplitude that has been obtained at $45°$ compare to $0°$, since the incident and reflected angles corresponded to the specular direction at $45°$. Pathloss has been calculated from equation 7, where N is the value of the sweep points and $\overline{H(f)}$ is the average (i.e., 10 snap shots) transfer function of the channel.

$$PL(dB) = -10\log_{10}\left[\frac{1}{N}\sum_{i=1}^{N}\left|\overline{H(f_i)}\right|^2\right] \quad (7)$$

Each measured reflection coefficient was obtained by using (8) with the associated measured received power ($P_r(dBm) = P_t(dBm) - PL(dB)$) and values of D_1, D_2 and D_{LOS}.

$$\{|\Gamma_\parallel|, |\Gamma_\perp|\} = \frac{D_1 + D_2}{D_{LOS}}\sqrt{\frac{Pr_{REF}}{Pr_{LOS}}} \quad (8)$$

Table I gives the predicted Fresnel reflection coefficients with the measured values. Measured values exhibited additional losses of reflected signals from the wall and the floor compared to smooth surfaces. It is useful to point out that the average pathloss difference between LOS and reflected signals for the

TABLE II
PATHLOSS DIFFERENCE VALUES OF WALL AND FLOOR IN dB.

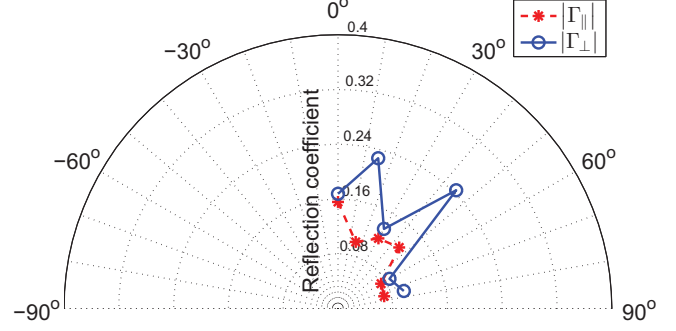| Surface	PL($|\Gamma_\parallel|$)		PL($|\Gamma_\perp|$)	
	Min	Max	Min	Max
Wall	18	23	13	21
Floor	16	22	11	26

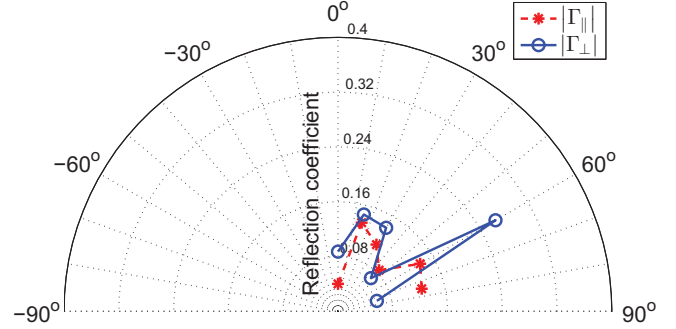Fig. 8. Measured reflection coefficients for the wall surface.

Fig. 9. Measured reflection coefficients for the floor surface.

wall and for the floor is found to be around 19 dB and the maximum and minimum values of the pathloss differences are listed in table II. The measured values of D_1 and D_2 and PL differences at each θ_i, have significant impact on reflection coefficient measurements. For example, in case of $|\Gamma_\perp|$ of the wall surface, the $D_1 + D_2$ value lies between around 2.08 m to 2.5 m, if PL difference is low at a particular θ_i and the $|\Gamma|$ value will experience higher value. Figs. 8 and 9 show the measured reflection coefficients for perpendicular and parallel polarization for wall and floor surfaces with different incident angles of θ_i, respectively. According to the surface height measurements of the wall surface (large scale range, i.e., $1.5\,m \times 5\,m$ area) with 10 cm grid spacing, the σ_h and T were found to be 6 cm and 84 cm, respectively [12]. The wall surface consists of a bunch of tilted rock plates (with maximum heights much higher than the wavelength) and sharp rock edges. However, in small scale area ($50\,mm \times 50\,mm$), it is assumed that the wall surface consists of tangent planes with a roughness less than λ and a correlation length much greater than λ. This may produce strong reflections (specular) as well as strong scattered (non specular) signals. Measurement results show high fluctuations of the reflection coefficient and strong
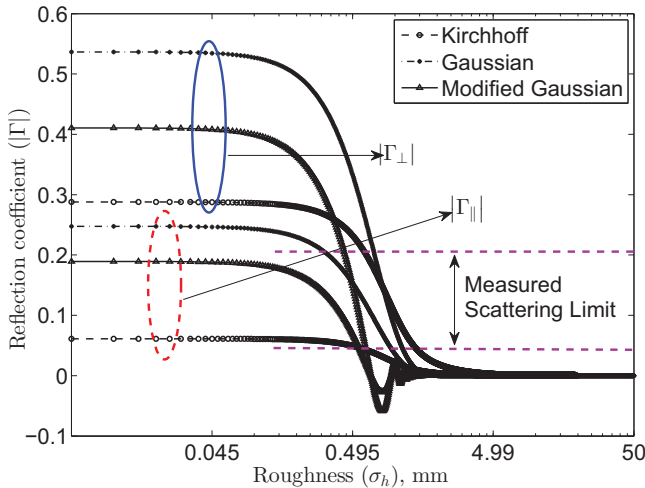
Fig. 10. Predicted reflection coefficients for the wall surface.

reflections. With zero σ_h, the $|\Gamma|$ is independent of the λ. In the considered environment, the wall surface has a σ_h, exhibiting reflection coefficients that are functions of the λ. According to Kirchhoff theory, if $T \gg \lambda$, the reflections will be in specular directions. If $T > \lambda$, more diffuse components will be produce across specular directions. If the value of σ_h is constant at a particular incident angle in a given area, either it has $T > \lambda$ or $T \gg \lambda$, the maximum amplitude of reflection coefficients remains constant. Fig. 10 shows the predicted $|\Gamma|$ for the considered surface material (i.e. granite) of the wall with $\theta_i = 45°$ and $T = 10\lambda$, considering the roughness between 0 to 50 mm. According to the predicted reflection coefficients and the measured scattering limit (between maximum and minimum value) of the wall, the appropriate scattering model can be chosen for the wall surface.

On the other hand, the floor was mostly flat and filled with mud containing small rocks. By considering a small scale area ($50\,mm \times 50\,mm$), it may also assumed that, σ_h is less than λ and the value of T is higher than the wall surface height. Measurement results show strong reflections mostly in specular directions and low scattering in non specular ones. Less variability of $|\Gamma|$ compared to the wall has been observed due to the fact of lossy surface (which absorbs power), and its structural characteristics and higher correlation length of surface heights. Since the measured scattering limit of $|\Gamma|$ for the floor (with both polarizations) in specular and non specular directions is between 0.0591 to 0.2656 (as shown in Fig 9), it can be modelled with one of the scattering models used for the wall as shown in Fig. 10. Girders and pipes may have significant scattering effect on the propagation, since the directional antennas have $12°$ HPBW, however, no effect has been observed during the measurements because they were outside the propagation area.

V. CONCLUSION

In this paper, the reflection coefficients in an underground mine wall and floor surfaces have been measured and intended to find possible scattering models. According to the results, specular reflections of the wall and floor are strong and scattering phenomena has been found in non specular directions. This scattering phenomena exhibits to choose an available appropriate scattering model for the mine surface. Moreover, a wall surface of the mine is more reflective and scattered than lossy floor surface. The results can be used for scattered channel modelling purpose. Further investigations may be carried out to determine the reflection coefficients associated with mine floors, walls and ceilings into different frequencies and different areas and make a statistical distribution.

REFERENCES

[1] S. K. Yong, P. Xia, and A. V. Garcia, *60 GHz Technology for Gbps WLAN and WPAN: From Theory to Practice*. Wiley, 2011.

[2] O. Landron, M. J. Feuerstein, and T. S. Rappaport, "Comparison of theoretical and empirical reflection coefficients for typical exterior wall surfaces in a mobile radio environment," *IEEE Transactions on Antennas and Propagation*, vol. 44, no. 3, pp. 341 – 351, 1996.

[3] H. Zhao, R. Mayzus, S. Sun, M. Samimi, J. K. Schulz, Y. Azar, K. Wang, G. N. Wong, F. Gutierrez, and T. S. Rappaport, "28 GHz millimeter wave cellular communication measurements for reflection and penetration loss in and around buildings in new york city," in *IEEE International Conference on Communications*, Budapest, Hungary, 2013, pp. 5163 – 5167.

[4] J. Ahmadi-Shokouh, S. Noghanian, and H. Keshavarz, "Reflection coefficient measurement for north american house flooring at 57-64 GHz," *IEEE Antennas and Wireless Propagation Letters*, vol. 10, pp. 1321 – 4, 2011.

[5] K. Sato, T. Manabe, T. Ihara, H. Saito, S. Ito, T. Tanaka, K. Sugai, N. Ohmi, Y. Murakami, M. Shibayama, Y. Konishi, and T. Kimura, "Measurements of reflection and transmission characteristics of interior structures of office building in the 60-GHz band," *IEEE Transactions on Antennas and Propagation*, vol. 45, no. 12, pp. 1783 – 92, 1997.

[6] B. Langen, G. Lober, and W. Herzig, "Reflection and transmission behaviour of building materials at 60 GHz," in *5th IEEE International Symposium on Personal, Indoor and Mobile Radio Communications (PIMRC'94)*, vol. 2, 1994, pp. 505 – 9.

[7] E. Violette, R. Espeland, R. DeBolt, and F. Schwering, "Millimeter-wave propagation at street level in an urban environment," *IEEE Transactions on Geoscience and Remote Sensing*, vol. 26, no. 3, pp. 368–380, May 1988.

[8] A. Maltsev, R. Maslennikov, A. Sevastyanov, A. Khoryaev, and A. Lomayev, "Experimental investigations of 60 GHz WLAN systems in office environment," *IEEE Journal on Selected Areas in Communications*, vol. 27, no. 8, pp. 1488–1499, October 2009.

[9] C. Lounis, N. Hakem, G. Delisle, and Y. Coulibaly, "Large-scale characterization of an underground mining environment for the 60 GHz frequency band," in *2012 International Conference on Wireless Communications in Underground and Confined Areas, ICWCUCA 2012*, Clermont-Ferrand, France, 2012, pp. 314 – 17.

[10] T. Rappaport, *Wireless communications: principles and practice*, ser. Prentice Hall communications engineering and emerging technologies series. Prentice Hall PTR, 2002.

[11] P. Beckmann and A. Spizzichino, *The Scattering of Electromagnetic Waves from Rough Surfaces*, ser. International Series of Monographs on Electromagnetic Waves. Pergamon Press, 1963.

[12] S. Tariq, C. Despins, S. Affes, and C. Nerguizian, "Rough surface scattering analysis at 60 GHz in an underground mine gallery," in *2014 IEEE International Conference on Communications Workshops (ICC)*, Sydney, Australia, June 2014, pp. 724–729.